Heliyon 8 (2022) e11698

Contents lists available at ScienceDirect

Heliyon

journal homepage: www.cell.com/heliyon

Research article

Noninvasive blood oxygen, heartbeat rate, and blood pressure parameter monitoring by photoplethysmography signals

Chin-Jung Ku [1], Yuhling Wang [1], Chia-Yu Chang, Min-Tse Wu, Sheng-Tong Dai, Lun-De Liao [*]

Institute of Biomedical Engineering and Nanomedicine, National Health Research Institutes, No 35, Keyan Road, Zhunan Town, Miaoli County 350, Taiwan

ARTICLE INFO

Keywords:
Continuous blood pressure
Noninvasive
Photoplethysmography
MIMIC-II database

ABSTRACT

The popularization of long-term invasive tools for continuously monitoring blood pressure remains challenging. However, with the rising popularity of wearable personal health management devices, non-cuff blood pressure measurement technology that applies electrocardiography (ECG) and photoplethysmography (PPG) has gradually received increasing attention. In particular, whether blood pressure can be measured continuously by the PPG signal alone is of great interest. In this study, we aim to develop a device that includes systolic and diastolic blood pressure calculation formulas derived from characteristic waveform points in the PPG time domain and that can measure blood oxygenation and heart rate. This device applies empirical formulas developed by PPG waveforms in the PhysioNet MIMIC-II database to calculate blood pressure. The systolic and diastolic pressures are then compared with the actual blood pressures obtained from invasive blood pressure waveforms to verify the effectiveness and feasibility of the complete developed system. Overall, 263 waveforms with double peaks and 261 waveforms with only a single peak totaling 524 sets of data are used to derive the empirical formulas. The systolic blood pressure estimation result using single peak analysis has an excessively large error exceeding ±40 mmHg, providing no reference value. However, systolic blood pressure estimation is notably better in double peak analysis, with error values reducing to approximately 23 mmHg. Diastolic pressure estimation errors are low with both single (±7 mmHg) and double peak (±4 mmHg) analyses. The error is lower in double-peak analysis than in single-peak analysis for obtaining systolic pressure from PPG waves. We plan to use PPG to detect additional physiological parameters in the future, e.g., respiratory rate, heart rate variability, or irregular heartbeat, to further enhance the functionality of PPG-based wearable devices.

1. Introduction

When assessing personal physical health, the heart rate, blood pressure, body temperature, and respiration rate are the most suitable parameters for rapid measurement and are also the most important indicators of health [1]. Although there are many convenient and inexpensive medical instruments on the market, the values of these physiological parameters can be easily measured by noninvasive methods [2, 3]. However, there is still no ideal and suitable tool available to achieve continuous, long-term monitoring. For example, only invasive manometers can be used if users wish to continuously and accurately measure blood pressure changes. Among the associated parameters, especially for systolic blood pressure and diastolic blood pressure, long-term abnormal changes are often early warning signs of diseases in many body organs [4].

The traditional method for measuring blood pressure is to use a mercury sphygmomanometer or the oscillometric method commonly used in modern electronic sphygmomanometers. Regardless of the method, it is necessary to pressurize and deflate a pressure cuff to measure a single systolic and diastolic blood pressure. In addition to the cumbersome and time-consuming operation, the main problem is that it cannot be performed for continuous real-time detection. With the increasing popularity of wearable personal health management devices, nonpulse-belt blood pressure measurement technology has gradually received attention, and new theories and ideas have emerged. Among these techniques, the approach of measuring and estimating blood pressure by using the time or phase difference between the electrocardiography (ECG) and photoplethysmography (PPG) signals is proposed and implemented [5, 6]. Although this method cleverly solves the shortcoming of only one-time, intermittent blood pressure measurement,

* Corresponding author.
E-mail addresses: ldliao@nhri.edu.tw, gs336.tw@gmail.com (L.-D. Liao).
[1] Chin-Jung Ku and Yuhling Wang contributed equally to this paper.

https://doi.org/10.1016/j.heliyon.2022.e11698
Received 9 May 2022; Received in revised form 2 August 2022; Accepted 10 November 2022

due to the electrode patch that needs to be worn to capture the ECG signal, there is still discomfort caused by the long-term contact of the patch with the skin. In addition, the entanglement of electrode leads also indirectly affects the convenience of use. Because of the PPG measuring device's inherently easy-to-use and straightforward characteristics and the associated convenience and comfort of wearing, measure blood pressure continuously using the PPG signal alone is proposed [7, 8].

The theory of predicting blood pressure with the PPG signal alone is derived from the time difference relationship between the ECG signal and the PPG signal, similar to early derivations [9], and there is also a model that uses a neural network to extract the eigenvalues of the PPG signal for training directly [10, 11]. Some theories are based on the original waveform of the time-domain PPG signal in addition to the first-order or even the second-order derivative waveform [12]. There is also a correlation between the amplitude and the wave height obtained from the complete waveform shape (such as the time value corresponding to the wave height percentage of the time percentage) [13]. The corresponding wave heights are based on the associated eigenvalues. Alternatively, we can combine the above theories and directly incorporate them into a neural network for training to obtain a model to predict [14, 15]. However, excessive reliance on neural networks is unsatisfactory. Although the model obtained by training has excellent prediction results for the existing training data, the results are different if a new dataset is added unless the model is retrained [16]. It is difficult to recognize the uniqueness of the individual unless a corresponding individual model is trained separately, but this is impractical and violates the original strategy of universally applying a standard model [17].

Based on the various factors discussed above, we choose the relevant literature on the systolic and diastolic blood pressure calculation formulas derived from the waveform characteristic points in the PPG time domain with a partial theoretical basis as the starting point for this study [18, 19]. First, the self-developed hardware circuits, firmware, and software programs to calculate blood pressure are reviewed. Then, with the synchronization data (i.e., invasive blood pressure waveforms and PPG signal waveforms) obtained and filtered from the PhysioNet MIMIC-II database, we identify the characteristic points of the waveform, apply an empirical formula to calculate the systolic and diastolic blood pressure, and then compare the systolic and diastolic blood pressure with the actual blood pressure obtained from the invasive blood pressure waveform to verify the effectiveness and feasibility of the overall system. Finally, the difficulties and problems faced in implementation steps are discussed in the context of the device and method developed in this study aiming to find more effective, feasible, and comprehensive solutions.

2. Materials and methods

2.1. PPG measurement and analysis system

Regarding oxygen concentration measurement in blood, PPG signals based on body tissues naturally have a low absorption rate for red light and near-infrared light. In contrast, red blood cells have a high absorption rate for near-infrared light; combining these two characteristics, the difference in absorption rates can be used to derive the oxygen concentration carried by red blood cells. As shown in Figure 1A, red light and near-infrared LED light are used to irradiate the finger. After the light enters the body tissue and is absorbed, the photodiode receives the remaining reflected light, and the intensity is measured to compare the absorption of the two types of light. In addition, the light-penetrating measurement method is also feasible, and the difference is only in the placement of the photodiode and the short path for the light to pass through. This kind of design of the mechanism is also inconvenient; however, it is usually better to use the reflective approach. Figure 1B displays a schematic diagram of the light path of different wavelengths after entering the body tissue.

Note that the penetrating ability of near-infrared light with longer wavelengths in the figure is also higher than that of red light; thus, the former can reach the depths of the tissue and become absorbed by red blood cells in the blood. Therefore, it can better reflect the changes in blood flow in the blood vessels. When we need to detect blood oxygen concentrations, both light sources are needed; however, when we wish to use the PPG waveform to estimate blood pressure values, it is natural to obtain helpful information from the PPG waveform of near-infrared light that can faithfully reflect blood flow conditions. Figure 1C demonstrates the relative relationship between the PPG waveform and the ECG waveform. Figure 1D shows a typical dual-peak PPG waveform, as described in detail in Section 2.3.

To capture the PPG waveform of near-infrared light, we assemble a set of basic blood oxygen measurement systems as a tool for research and experimentation, including red and near-infrared LED light sources, photodiode receivers, photoelectric system control chip circuits, and control firmware programs, using the MAX30101 module produced by Maxim as a front-end sensor to capture PPG signals. For a highly integrated Arduino module (Arduino Nano 33 BLE), we set the operating mode of the MAX30101 module through the SPI communication interface, receive the PPG waveform that has been converted into an electrical signal, and transmit the PPG waveform to the individual through the low-power Bluetooth interface (BLE) to the computer. A standard rechargeable 850 mAh lithium polymer battery powers the developed system to reduce the interference caused by noise that can distort the PPG waveform. The battery can be charged with the TP4056 charging module via USB power. The software program on the personal computer preprocesses the original PPG waveform and then extracts the correlation of the near-infrared PPG waveform. A self-developed algorithm analyzes the information to calculate the predicted systolic and diastolic blood pressure. The main components of the overall system and the assembled prototype are described in Figure 2A and 2B. In addition to capturing the PPG waveform from near-infrared light for blood pressure calculation, the prototype of the test system can also measure and calculate the blood oxygen concentration and heart rate of the measured subject.

2.2. MIMIC-II database and data classification and processing methods

In addition to circuit and analysis software development, to meet the needs of developing and verifying the algorithm for calculating blood pressure from PPG waveforms, a ready-made and suitable waveform file from the PhysioNet MIMIC-II database is used as the target for testing. This MIMIC-II database has synchronized PPG waveforms and invasive blood pressure waveforms to fit this study's goal. Details are shown in the block diagram in Figure 3A. First, a self-written command program is used to download the PPG waveform recording file (sometimes called the PLETH waveform in the database). Then, from these downloaded files, after removing the recording files whose duration is too short, we convert the files into.txt or.csv format and export them. Second, through manual inspection and selection, we eliminate the artificial noise segment caused by the action factor (motion artifact). Then, the typical waveform of approximately 30 s is extracted from each record file. Finally, the PPG waveform data are stored in the original state as a file, and the ambulatory blood pressure (ABP) waveform is processed in advance to obtain systolic and diastolic blood pressure for each blood pressure wave and then saved as the gold standard for actual blood pressure values. Figure 3B is the interface for previewing the waveforms from the database provided by MIMIC-II. Figure 3C and 3D are examples of typical ABP and PPG waveforms obtained after processing from the step in Figure 3A. For the method of calculating the systolic and diastolic blood pressure from the ABP waveform, the first step is to separate each independent pulse wave and then find the maximum value of the pulse wave, which is the corresponding systolic blood pressure. Then, the minimum value of the pulse wave is found, which is equivalent to the value of diastolic blood pressure. After the above processing steps, we obtain a total of 48 available waveforms of 30 s each, including 22 waveform sets with double peaks and 26 waveform sets with only a single peak. Based on the number of complete waveforms available for analysis and the

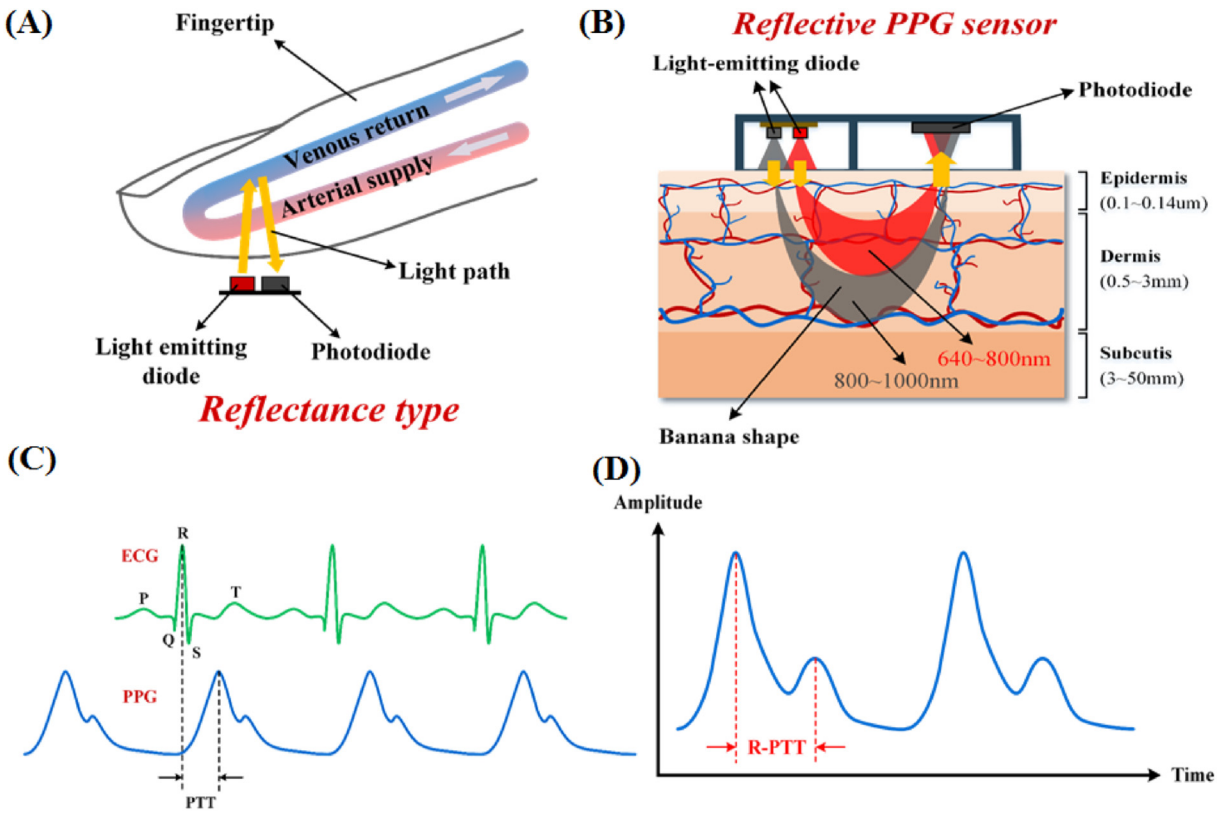

Figure 1. (A) Red light and near-infrared LED light are used to irradiate the finger. After the light enters the body tissue and is absorbed, the photodiode receives the remaining reflected light, and the intensity is measured. In this way, the absorption degree of the two kinds of light is compared. (B) Schematic diagram of the light path of different wavelengths after entering the body tissue. Note that the penetrating power of near-infrared light with longer wavelengths in the figure is also higher than that of red light, so the former can reach the depths of the tissue and become absorbed by red blood cells in the blood so that it can reflect changes in blood flow in the blood vessels. (C) The relative relationship between the ECG signal waveform and the PPG signal waveform in terms of characteristics and the phase difference between the two, the R wave of the ECG, and the main peak of the PPG also show a one-to-one correspondence. (D) The R-PTT is equivalent to the time interval between two peaks, exhibiting the standard double-peak PPG waveform.

corresponding ABP blood pressure values, there are a total of 263 waveforms with double peaks and 261 waveforms with only a single peak, which is equivalent to 524 sets of data. After the blood pressure calculation algorithm is verified using these archives, the previously designed basic blood oxygen measurement system is used to measure PPG and calculate blood pressure under actual conditions to thoroughly verify whether the results are as expected by this study.

2.3. PPG data analysis method

Noted that the informed written consent was provided by all participants before the experiment. This study was approved by the National Health Research Institutes, Taiwan. All procedures performed in this study involving human participants were in accordance with the ethical standards of the National Health Research Institutes, Taiwan. The raw data extracted from the MIMIC-II database are analyzed through the processing procedures and steps shown in Figure 4. First, the components of the signal baseline drift are removed to obtain a stable waveform. Small-amplitude moving average processing is applied to filter out useless high-frequency noise and separate the PPG pulse wave segment corresponding to a single heartbeat. Then, the PPG pulse wave segment corresponding to a single heartbeat is divided. Next, it is determined whether the single pulse wave belongs to the type with only a single peak or whether it belongs to the type with multiple peaks. For waveforms with numerous peaks in the pulse wave, the relevant parameters for calculating blood pressure can be directly obtained by measuring the relationship between the characteristic points of the waveform in the time domain of the PPG waveform. The relevant parameters for calculating blood pressure are obtained directly from the relationship between the usual points of the waveform in the time domain of the measured PPG waveform.

Figure 1C illustrates the relative relationship between the ECG signal waveform and the PPG signal waveform in terms of characteristics. In addition to the phase difference between the two, the R wave of ECG and the main peak of PPG also show a one-to-one correspondence, which is inevitable. As a result, because the signal source is the same, it is only after the modulation of various body parts that it appears different. Of course, the exceptions caused by arrhythmias are another matter, and this topic is not considered in this paper. Excluding arrhythmic pulse waves from PPG waveforms may be an additional research topic. The pulse transit time (R-PTT) concept is used on the PPG waveform to estimate blood pressure for this relative relationship. As seen in Figure 1D, a standard double-peak PPG waveform is taken as an example, and R-PTT is equivalent to the time interval between two peaks. For a PPG waveform with an unclear second peak or only a single peak, the R-PTT value still exists, but it must be obtained indirectly in other ways, such as with the quadratic derivative waveform, as reviewed later regarding the details and discussion of the impact on blood pressure calculations. The R-PTT is based on two formulas (Eqs. (1) and (2)) as follows:

$$DBP = K_b + \frac{2}{0.031} \cdot ln\frac{K_c}{R - PTT} - \frac{1}{3} \cdot \frac{K_a}{R - PTT^2} \quad (1)$$

$$SBP = DBP + K_a \cdot \frac{1}{R - PTT^2} \quad (2)$$

K_a, K_b, and K_c are fixed parameters obtained after correction from the

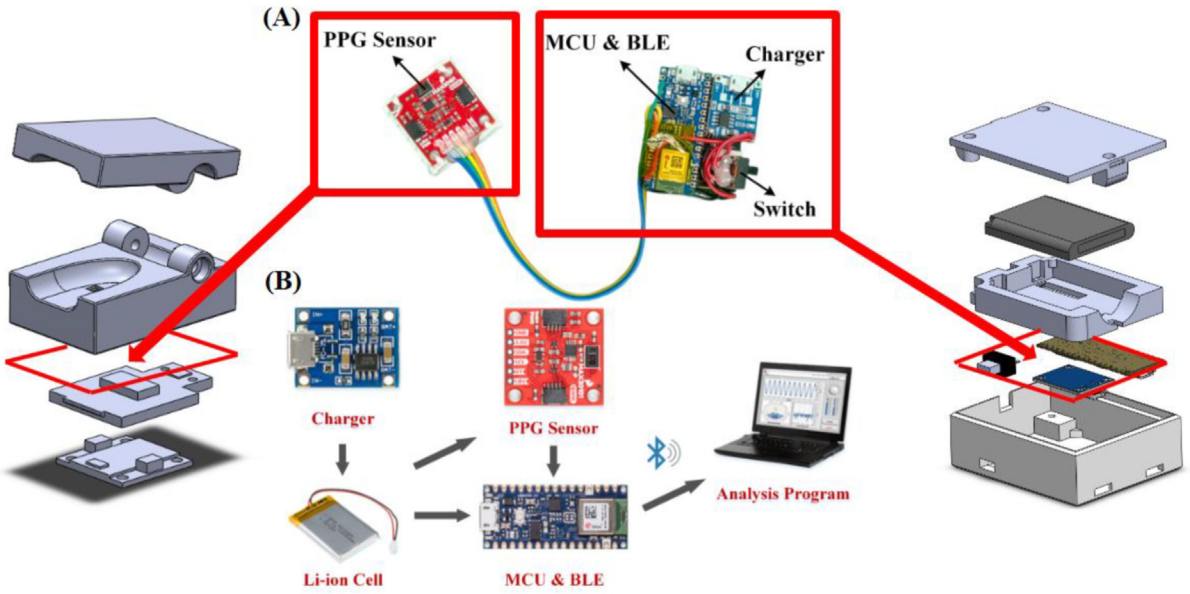

Figure 2. To capture the PPG waveform of near-infrared light, we assemble a set of basic blood oxygen measurement systems as a tool for research and experimentation, including red and near-infrared LED light sources, photodiode receivers, photoelectric system control chip circuits, and control firmware programs, using the MAX30101 module produced by Maxim as a front-end sensor to capture PPG signals. For a highly integrated Arduino module (Arduino Nano 33 BLE), we set the operating mode of the MAX30101 module through the SPI communication interface, receive the PPG waveform that has been converted into an electrical signal, and transmit the PPG waveform to the individual through the low-power Bluetooth interface (BLE) to the computer. A standard rechargeable 850 mAh lithium polymer battery powers the developed system to reduce the interference caused by noise that would distort the PPG waveform. The battery can be charged with the TP4056 charging module via USB power. The software program on the personal computer is responsible for preprocessing the original PPG waveform and then extracting the correlation of the near-infrared PPG waveform. A self-developed appropriate algorithm then analyzes the information to calculate the predicted systolic and diastolic blood pressure. (A) Assembled prototype. (B) Main components of the system. The analysis platform can be a personal computer or a Raspberry Pi single-board microcomputer.

experimental results according to personal conditions. Therefore, our method is to first measure the current systolic blood pressure and diastolic blood pressure and then obtain the simultaneous R-PTT value with the arm sphygmomanometer. Next, the above formulas are applied to obtain the set of K_a, K_b, and K_c values. Finally, the systolic blood pressure and diastolic blood pressure for a subsequent period of continuous time can be obtained by substitution into the above formula according to the change in R-PTT. For the data retrieved from the MIMIC-II database, the real systolic and diastolic blood pressures are stored as files, as seen in Figure 3, which can be directly used to solve for K_a, K_b, and Kc in the formula. Finally, as the last step displayed in Figure 4, the existing blood pressure value in the database is used as the absolute standard for comparison to verify the algorithm's accuracy.

3. Results

3.1. System performance and stability test

Using the prototype assembled in Figure 2A, with the waveform receiving and analysis program on the computer (such as the actual operation image in Figure 5), the current subject's PPG waveform can be displayed in real-time, and the systolic blood pressure and systolic blood pressure of the current analysis result can be obtained. The related details are explained in detail in Section 3.2. The results of the static MIMIC-II data analysis are first presented here. First, the analysis results obtained when the self-developed software algorithm is applied to the data extracted from the MIMIC-II database are presented. Some PPG waveforms have multiple peaks, while the second peak of some PPG waveforms is unclear or the waveform has only a single peak. Therefore, the objects of analysis are also divided into two groups: 1) a lack of two or more prominent peaks and 2) two sets of data with more than two distinct peaks.

As shown in Figure 6A, 6B, 6C, and 6D, the diastolic blood pressure and systolic blood pressure obtained by the PPG analysis of a single peak are the analysis results relative of the actual blood pressure value. The Bland-Altman analysis toolbox provided by MATLAB software [20, 21] was used to generate the plots for Figure 6B and 6D, and subsequent figures were generated in the same way. The distribution of actual systolic blood pressure of the subjects is between 92 and 174 mmHg, while the distribution of actual diastolic blood pressure is between 44 and 85 mmHg. According to the distribution diagram of the comparison between the estimated value of the diastolic blood pressure and the actual blood pressure value in Figure 6A, the calculation results are generally satisfactory. According to the Bland-Altman diagram of diastolic blood pressure in Figure 6B, most of the error values are concentrated in the vicinity of plus or minus 7 mmHg Figure 6C shows the distribution of the estimated systolic blood pressure value and the actual blood pressure value; since the test data are all from critically ill intensive care unit (ICU) patients, the second wave peak is challenging to evaluate, resulting in considerably scattered results. In addition, the systolic blood pressure is shown in Figure 6D. The Bland-Altman diagram also reveals that the systolic blood pressure estimation result of a single peak has an error that is too large; the error value exceeds plus or minus 40 mmHg, which basically has no reference value. For the PPG waveform with only a single peak, if even the naked eye cannot identify the existence of any second wave, the analysis method adopted in this paper cannot be applied.

Next, the data shown in Figure 7A, 7B, 7C and 7D are the diastolic blood pressure and systolic blood pressure obtained by the PPG analysis with a prominent second peak. The actual systolic blood pressure distribution of the subjects is between 104 and 185 mmHg, while the actual diastolic blood pressure is between 36 and 84 mmHg. The analysis results are relative to the actual blood pressure value. The distribution diagram of the estimated diastolic blood pressure and the actual blood pressure value in Figure 7A indicate that the estimated value is quite close to the

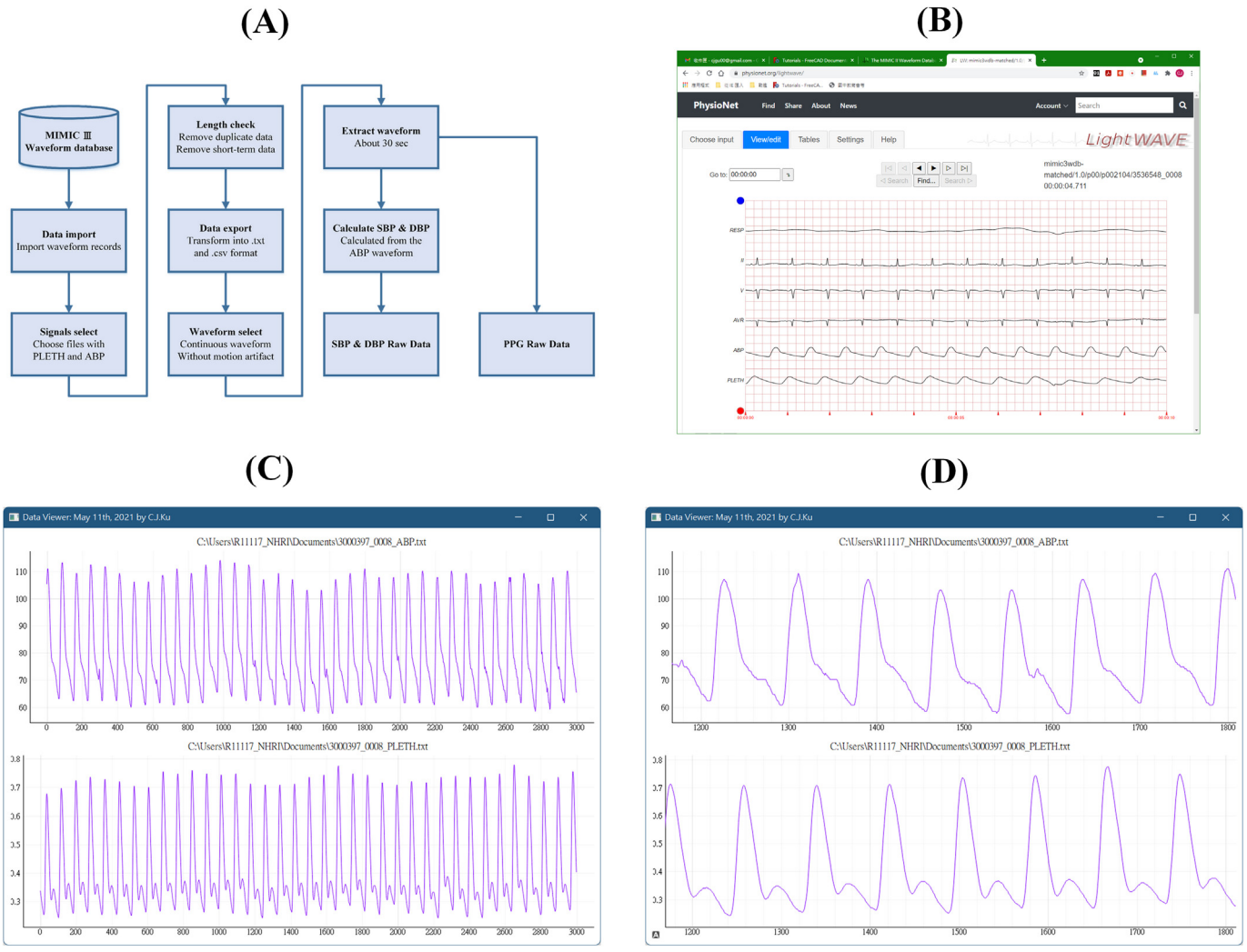

Figure 3. Block diagram of the MIMIC-II database and data classification processing method. (A) The flowchart block diagram for the data preprocessing. The data, including PPG and invasive blood pressure synchronization waveforms, are selected from the large amount of data in the database. Next, the data series with a length that is longer than 30 s are further screened out, and then the waveform files in txt and CSV formats are exported. Then, the artifact fragments caused by the subject's actions are removed by manual inspection, and a steady-state waveform of approximately 30 s is captured for each record. After the above processing steps, we obtain a total of 48 available waveforms of 30 s each, including 22 waveform sets with double peaks and 26 waveform sets with only a single peak. Based on the number of complete waveforms available for analysis and the corresponding ABP blood pressure values, there are a total of 263 waveforms with double peaks and 261 waveforms with only a single peak, which is equivalent to 524 sets of data. Finally, the PPG waveform is directly output for subsequent analysis by the analysis program. In contrast, the invasive blood pressure waveform first calculates the systolic and diastolic blood pressure corresponding to each pulse wave and then exports it for subsequent analysis by the analysis program. (B) The preview interface for the waveform from the MIMIC-II database. (C) Example of typical ABP (top half) and PPG (bottom half) waveforms after preprocessing. (D) Enlarging part of the waveform in (C) to show its details, as seen in the figure, the PPG waveform slightly lags behind the ABP waveform, which is an inevitable phenomenon, because the change of blood oxygen must be slower than that of the pulse wave, so there is a time difference delay. This factor has been considered when analyzing the waveform.

actual value. As seen in the Bland-Altman diagram of diastolic blood pressure in Figure 7B, most of the error values are concentrated within plus or minus 4 mmHg. In addition, the systolic blood pressure part refers to the distribution chart of the comparison between the estimated systolic blood pressure value and the actual blood pressure value in Figure 7C. The analysis results are notably better than the case of a single peak. In Figure 7D, the Bland-Altman diagram of systolic blood pressure shows that the error value is reduced to approximately 23 mmHg.

The empirical formula derived from the same theory and the same analysis algorithm is applied to these two data groups, but there are noticeable differences, and the estimated results are closely related to the shape of the PPG waveform when the mathematical formula is applied. Is there something wrong with the theory itself or do the differences arise from the differences in the measurement and analysis methods? This problem is addressed in subsequent sections to explain its causes and possible solutions.

3.2. Actual measurement results: blood oxygen/heartbeat/diastolic blood pressure/systolic blood pressure

The software and hardware systems are integrated and applied to the actual human test to compare with the analysis results from the developed software. Limited by practical factors, it is difficult to obtain a continuous synchronous blood pressure waveform, such as the MIMIC-II database during the real test. Therefore, the first systolic and diastolic blood pressure measurement methods are obtained by measuring the PPG waveform with a commercially certified OMRON blood pressure monitor (HEM-7155-E). In addition, to highlight the difference between the test results of the selected specific ethnic groups and the test results of the nonspecific general ethnic groups, the subjects of the real test are limited to the adolescent group between the ages of 20 and 30 years old and without special health problems. The study was conducted according to the guidelines of the Declaration of Helsinki. Moreover, almost all the

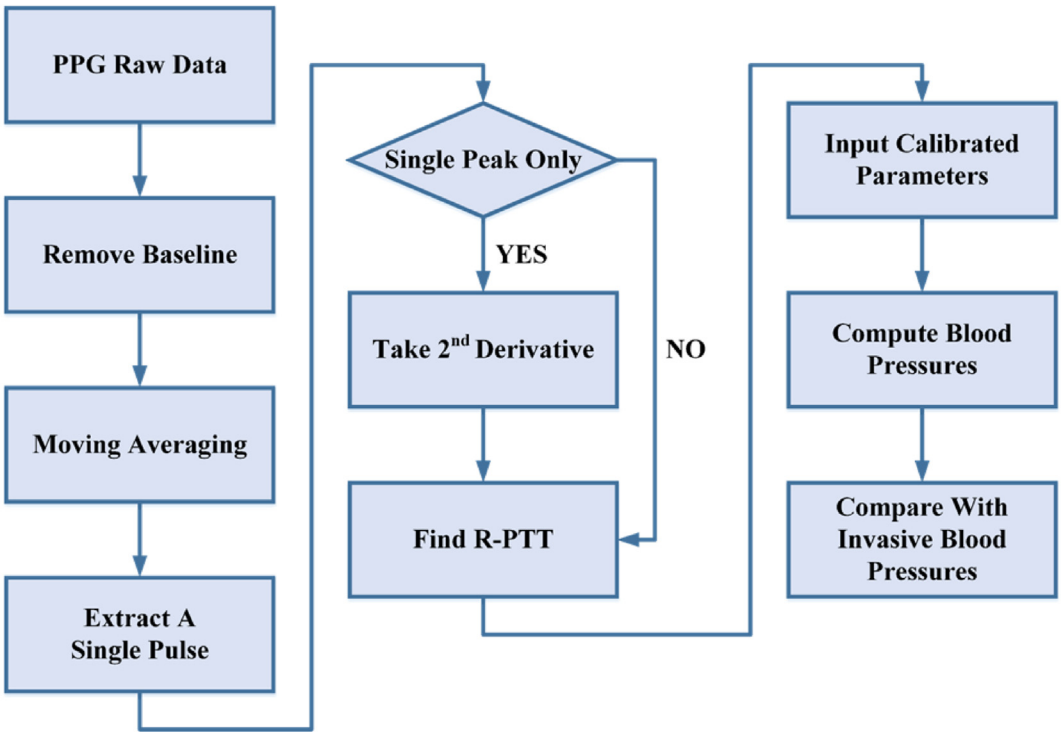

Figure 4. Raw PPG waveform data processing procedures, steps, and analysis methods. The original PPG waveform first needs to remove the DC component and the baseline component that causes the signal drift. Then, the noise is removed by moving the average method and then dividing the waveform to obtain individual pulse waveforms. If there is only a single peak, the second derivative function must be obtained, the position of the corresponding second peak must be found, and then the value of R-PTT can be calculated. The highest and second peaks are directly calculated for waveforms with more than two peaks. The distance of the high peak is the required R-PTT. Next, the blood pressure value corresponding to each pulse wave can be calculated using the R-PTT with the correction parameters calculated from the user's initial blood pressure value input. Finally, the calculated blood pressure value is compared with the invasive blood pressure value to verify the algorithm's accuracy.

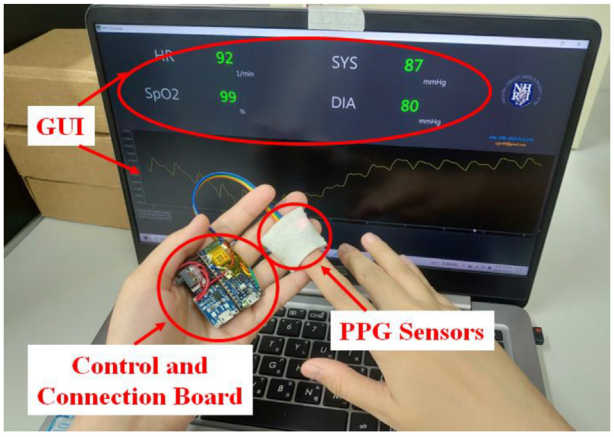

Figure 5. Configuration screen and actual operation of this system during testing. In addition to displaying the PPG waveform in real-time, the analysis program also displays the current heart rate, blood oxygen concentration, and systolic and diastolic blood pressure calculated by each pulse wave. Although a personal computer is used as a demonstration, since the calculation amount is not as large as that of a deep learning algorithm, even a Raspberry Pi single-board microcomputer or a single-chip MCU is suitable for porting to portable devices. For information about the operation mode and result presentation of this system, please refer to Movie S1 in the supplementary file.

PPG waveforms in this group have obvious second wave peaks that can be identified, and it is relatively easy to analyze the data. Since it is purely for comparison and the previous literature has performed extensive testing of this group, the number of real life test samples is not very large, and the total number of people for the test is approximately 20 times. The main purpose is to confirm this experiment. The produced system can obtain results consistent with previous literature so as not to be biased. Figure 5 depicts the configuration and actual operation of the system during testing. The PPG measurement device transmits the waveform to a personal computer or a Raspberry Pi single-board microcomputer through Bluetooth for analysis and calculation, and the real-time PPG waveform display can be seen in the middle of the screen. The upper part of the screen displays the heart rate, SpO_2, systolic blood pressure, and diastolic blood pressure obtained by PPG waveform analysis and calculation, and the bottom part displays the average value of R-PTT within 6 s and a warning or error message. From the elapsed time (10 s) of the PPG waveform on the screen and counting the number of pulse waves within this time, it can be immediately verified whether the heart rate value is correct. The PPG waveform displayed in real time can be used to manually check whether the state is stable during the measurement and observe whether there is arrhythmia and other phenomena, thus providing an excellent auxiliary tool. Smooth, continuous changes in the 4 physiological parameters are observed. If there is a need to watch the long-term change trend of each parameter in the future, this trend can also be displayed through the record file or switched on the main screen, which can be achieved by only slightly modifying the software program.

4. Discussion

4.1. Results of other notable papers and discussion of the differences with our experimental data

At present, among the papers that use only a PPG waveform without ECG data to estimate the blood pressure value, most directly capture the original PPG waveform or add the eigenvalues of the quadratic derivative waveform and then use a neural network to make the prediction. The

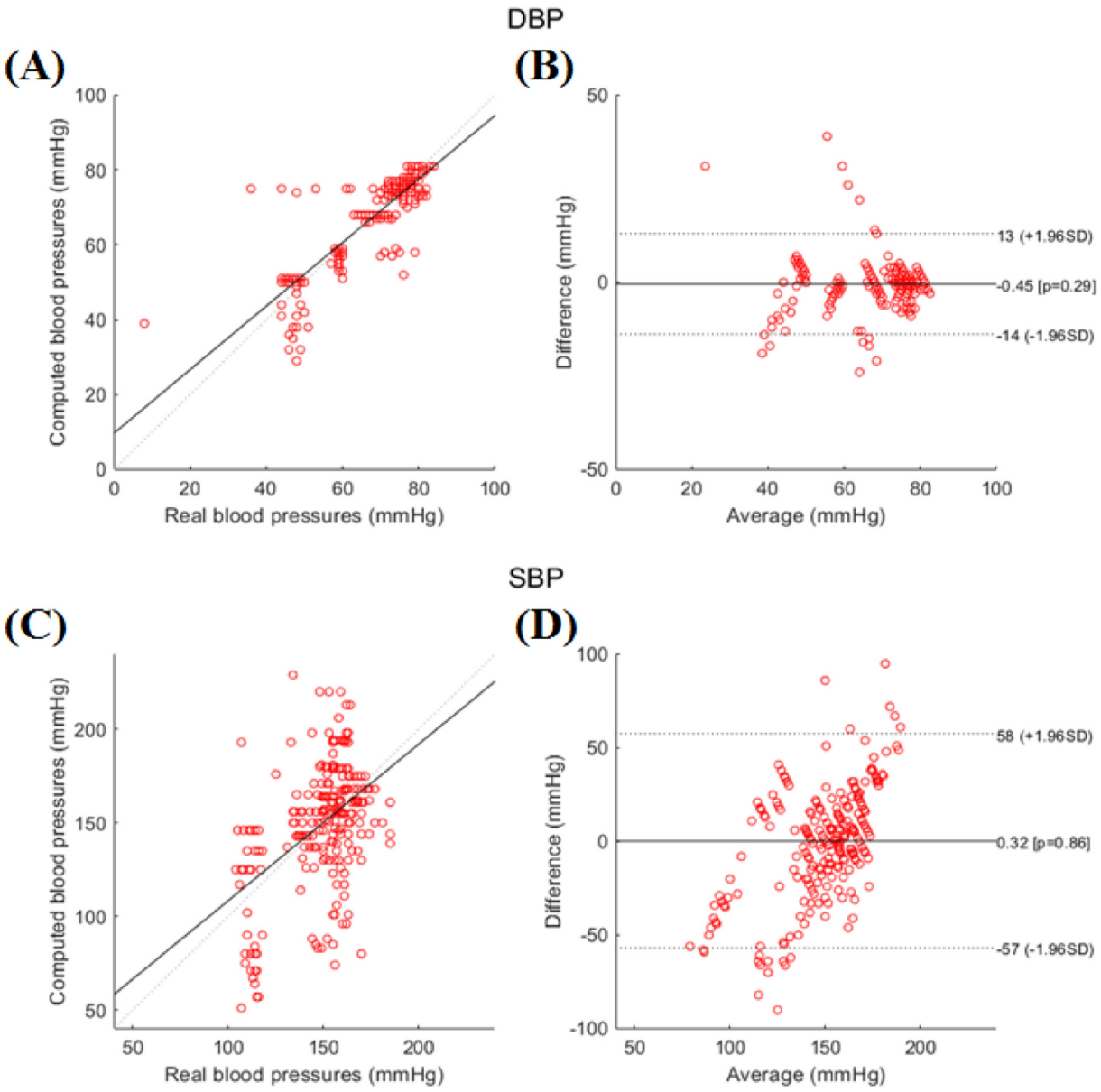

Figure 6. Single-peak PPG waveform analysis results. (A) Distribution diagram of the comparison between the estimated diastolic blood pressure and the actual blood pressure, which is approximately ideal. (B) Bland-Altman diagram of the diastolic blood pressure, most of which is concentrated at approximately 7 mmHg. (C) Estimated systolic blood pressure and actual blood pressure. Because the test data are the data of critically ill ICU patients, the second wave peak is challenging to evaluate, resulting in a considerably overdispersed result. (D) The Bland–Altman chart of systolic blood pressure has an excessively large error in the estimation results.

model obtained after learning and training is used to predict the blood pressure of new subjects and to have continuous blood pressure values for comparison. Most of the previous reports also used the waveform in the MIMIC-II database as the object of analysis [22, 23, 24]. However, the biggest problem of deep learning is that a vast amount of data is required for training to avoid the overfitting phenomenon of the model to ensure that the trained model has extremely high accuracy for the training data, but there are substantial errors in the actual test data. That is, the generality of the model must be improved through a large amount of training data rather than a unique model generated for a small amount of data. However, due to the limited data available in the MIMIC-II database, there are only thousands of data points from different cases. Therefore, the literature mentioned earlier is usually used only as training data for long-term measurement data of a few cases and naturally lacks generality. Few works in the literature have used actual measurement data [25, 26], but they also faced similar problems, and their approach was still based on long-term records to solve the problem.

In addition, the trained model must be verified against additional test data not included in the training data, and the result is the actual data. Many studies do not mention this part but use only the data of the training data as a result. Additionally, another problem is that most of these models do not consider the individual physiological characteristics, as mentioned in [15]. This is actually a very important factor, and even with the use of ECG with PPG and PTT to estimate blood pressure [27], the individual differences need to be considered. However, establishing a personal model for each individual is even more challenging.

A few papers are based on theoretical models and empirical formulas [28, 29, 30], and PPG waveforms or few feature points of quadratic derivative waveforms have been used to calculate blood pressure. The preliminary results are claimed to reach a considerable level, but almost all the subjects tested are concentrated in similar ethnic groups or are of similar age (mostly between 20 and 30 years old) or are healthy and disease-free. Moreover, their PPG waveforms are identical and perfectly show standard features. That is, they do not cover a wide range of levels,

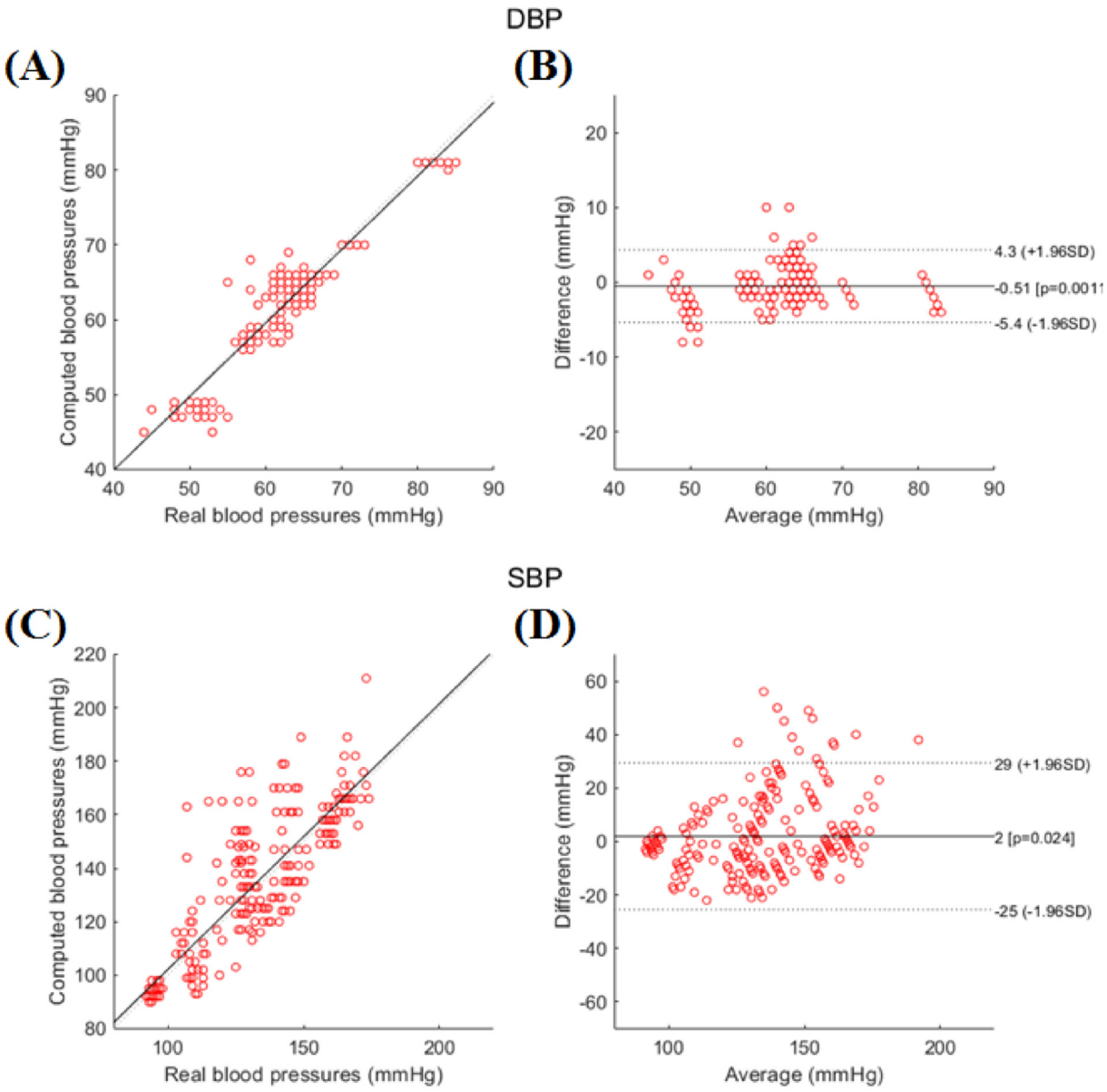

Figure 7. PPG waveform analysis results based on the clear second peak data. (A) Distribution of the estimated diastolic blood pressure and the actual blood pressure value. The restus values are very close. (B) Bland-Altman diagram of the diastolic blood pressure, most of which is concentrated at approximately 4 mmHg. (C) The estimated systolic blood pressure value is compared with the actual blood pressure value. The result is much better than the case of a single peak. (D) Bland-Altman diagram of systolic blood pressure; the error value is approximately 23 mmHg.

and test results for patients who need long-term monitoring are especially lacking.

To compensate for the above two deficiencies, the present paper deliberately selects different types of PPG waveforms to test the algorithm's effectiveness when retrieving PPG waveform data from the MIMIC-II database and aiming to cover broad types of age groups. Moreover, the MIMIC-II database was initially obtained from the ICU, and the subjects themselves all had some kind of disease or injury. During the actual testing, healthy people are included over different age groups. The database also covers most ethnic groups, thus enhancing its usefulness. Additionally, because no similar groups are deliberately selected for testing, the experimental results show that the analysis algorithm can achieve excellent results for certain groups, while the same algorithm would yield very different results for other groups.

For example, compared with the literature on the sample distribution that is similar to this experiment, for those with systolic and diastolic blood pressure covering a wide range, as in this experiment, the range of systolic blood pressure is 92–185 mmHg, and the range of diastolic blood pressure is 36–85 mmHg, mmHg, such as the data reported in a previous study [24, 31, 32]. This document uses a similar setting and blood pressure calculation method in this experiment, and the experimental results are quite similar (refer to Figure s9 in mentioned reference). The blood pressure error range is also substantially larger, which confirms that the experimental results do reflect the real situation but also face the same problem to be solved. Therefore, this paper uses machine learning to build a model and tries to postcorrect the data with the large original error, and the blood pressure error value is limited to within +/−15 mmHg. However, as mentioned above, using machine learning or deep learning models to analyze data has inherent problems. Although the data are beautiful, they obviously lack practicality.

In addition, compared with the literature [28], which was mainly referenced in this experiment, the test subjects of this literature are more concentrated in young healthy groups, and the blood pressure distribution range is not wide, which refers to similar individuals with little

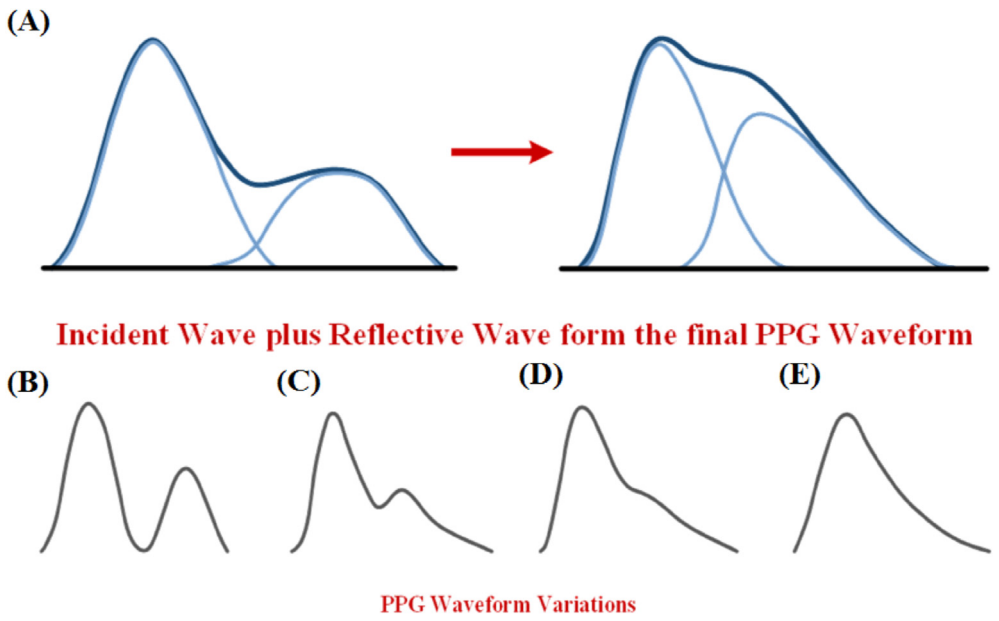

Figure 8. (A–B) The PPG waveform can basically be regarded as a composite wave formed by the fusion of the incident wave and the reflected wave. (C) Gradual merging of the incident wave and the wave crests. (D) In the second stage, the reflected wave crest gradually deforms, and only the turning point is visible. (E) In the third stage, the reflected wave characteristics almost disappear completely.

difference in the aforementioned conditions. The obtained experimental results are also quite good (refer to Figure s16 of the literature [28]), which is consistent with the results of the real test conducted in this experiment. It can be seen that the methods referenced and cited in this experiment have considerable limitations. If we wish to develop a continuous blood pressure measurement device that can truly be applied to most ethnic groups, there is still much improvement in the practice advocated by many papers.

4.2. Our system can be improved in the future

As mentioned in the analysis results in Section 3.1, the blood pressure value estimated by the PPG type with an apparent second peak is considerably more accurate than those of other approaches. The reasons for the formation of different types of PPG waveforms can be seen in Figure 8. The PPG waveform can basically be regarded as a composite wave formed by the fusion of the incident wave and the reflected wave (Figure 8A). The two clearly distinguishable wave peaks gradually merge together. The reflected wave peak gradually deforms in the second stage, and only the turning point is visible. When the wave finally enters the third stage, the reflected wave features almost entirely disappear. This phenomenon coincides with the typical PPG waveforms of various forms. In general, in healthy people and younger groups, the PPG waveform typically exhibits either the first or second stage (Figure 8A and 8B). The third stage waveform mainly occurs in elderly people with aging blood vessels and severely ill people (Figure 8C).

PPG waveforms of the first two forms provide a way to obtain the position of the second wave peak through an appropriate algorithm. The previous formula can also be used to estimate the blood pressure value with considerable accuracy. Because it is difficult to determine the position of the reflected wave, the estimated blood pressure value naturally deviates from the actual value by a large margin only in the last form (Figure 8D and 8E), which is also an opportunity for future improvement [33].

In addition, according to the actual experimental observation results, even if the subjective and objective conditions of the subjects are exactly the same and even if the wearing position of the PPG sensor is slightly changed, the PPG waveform is considerably different, changing between forms. This substantially increases the complexity of blood pressure estimation.

5. Conclusion

To develop a continuous blood pressure measurement device with practical properties, this study aims to integrate the most suitable software and hardware solutions from various existing technologies. At the application level, the attributes of light, thin and short are an inevitable trend, and thus, the use of a neural network-like approach seems inappropriate due to the high demand for computing power on the hardware and some inherent limitations of the algorithm. For a wearable device, the theoretically derived experimental formula is the focal point of this study. The limitations of the developed method and the system are discussed according to our actual test results via verification by extracting the available data from the MIMIC-II database. The main limiting factor comes from the shape of the PPG waveform, such as the typical double-peak waveform. The accuracy of the analysis is within approximately 23 mmHg for systolic blood pressure, and the error for diastolic blood pressure is within 4 mmHg, which is considered acceptable. However, for PPG waveforms with only a single peak due to severe illness, although the diastolic blood pressure error still falls within 7 mmHg, the systolic blood pressure error can be as high as 40 mmHg, which deviates from the practical value. Note that the data analyzed in many papers cover very limited ranges in both systolic and diastolic blood pressure, so the analysis results are quite ideal. The subjects analyzed in this paper had systolic blood pressures ranging from 92 to 185 mmHg and diastolic blood pressures ranging from 36 to 85 mmHg. Ideally, the experimental results correspond to practical applications as much as possible. The results of the actual measurement of a single healthy individual (that is, with a double-peak PPG waveform) from the prototype include a systolic or diastolic blood pressure error of less than 10 mmHg, but this cannot reflect the real situation. The reasons for the limitation and the strategies for future improvement are discussed, hoping to overcome this challenge to achieve the goal of real practicality. In addition, we hope to use PPG to detect additional physiological parameters in the future, such as, for example, respiratory rate, heart rate variability (HRV), or irregular heartbeat. In addition to integration into a multiparameter monitoring

tool, it may be possible to synthesize the relationship between various parameters to analyze more complex physiological phenomena, such as emotions.

Declarations

Author contribution statement

Chin-Jung Ku: Conceived and designed the experiments; Performed the experiments; Analyzed and interpreted the data; Contributed reagents, materials, analysis tools or data; Wrote the paper.

Chia-Yu Chang: Performed the experiments; Analyzed and interpreted the data; Contributed reagents, materials, analysis tools or data; Wrote the paper.

Yuhling Wang; Min-Tse Wu; Sheng-Tong Dai; Lun-De Liao: Contributed reagents, materials, analysis tools or data; Wrote the paper.

Min-Tse Wu; Sheng-Tong Dai; Lun-De Liao: Performed the experiments.

Yuhling Wang; Min-Tse Wu; Sheng-Tong Dai: Analyzed and interpreted the data.

Lun-De Liao: Conceived and designed the experiments.

Funding statement

This research was supported in part by the National Science and Technology Council of Taiwan through financial support under grant numbers 107-2221-E-400-002-MY3, 107-3111-Y-043-012, 108-2221-E-400-003-MY3 and 109-2314-B-400-037; by the National Health Research Institutes of Taiwan under grant numbers BN-111-GP-02; and by S & T grants from the Central Government of Taiwan under grant numbers 106-0324-01-10-05, 107-0324-01-19-02, 108-0324-01-19-06, 109-EC-17-A-22-1650 and 110-EC-17-A-22-1650.

Data availability statement

Data will be made available on request.

Declaration of interest's statement

The authors declare no conflict of interest.

Additional information

Supplementary content related to this article has been published online at https://doi.org/10.1016/j.heliyon.2022.e11698.

References

[1] C.T. Lin, C.Y. Wang, K.C. Huang, S.J. Horng, L.D. Liao, Wearable, multimodal, biosignal acquisition system for potential critical and emergency applications, Emerg. Med. Int. 2021 (2021), 9954669.
[2] Y.C. Tsao, F.J. Cheng, Y.H. Li, L.D. Liao, An IoT-based smart system with an MQTT broker for individual patient vital sign monitoring in potential emergency or prehospital applications, Emerg. Med. Int. 2022 (2022), 7245650.
[3] L.D. Liao, et al., Design and implementation of a multifunction wearable device to monitor sleep physiological signals, Micromachines 11 (7) (2020).
[4] E. Brophy, M. De Vos, G. Boylan, T. Ward, Estimation of continuous blood pressure from PPG via a federated learning approach, Sensors 21 (18) (2021).
[5] X.R. Ding, Y.T. Zhang, Pulse transit time technique for cuffless unobtrusive blood pressure measurement: from theory to algorithm, Biomed. Eng. Lett. 9 (1) (2019) 37–52 (in English).
[6] H. Gesche, D. Grosskurth, G. Kuchler, A. Patzak, Continuous blood pressure measurement by using the pulse transit time: comparison to a cuff-based method, Eur. J. Appl. Physiol. 112 (1) (2012) 309–315 (in English).
[7] R. Lazazzera, Y. Belhaj, G. Carrault, A new wearable device for blood pressure estimation using photoplethysmogram, Sensors 19 (11) (2019) (in English).
[8] H.H. Asada, P. Shaltis, A. Reisner, S. Rhee, R.C. Hutchinson, Mobile monitoring with wearable photoplethysmographic biosensors, IEEE Eng. Med. Biol. Mag. 22 (3) (2003) 28–40 (in English).
[9] A. Chandrasekhar, M. Yavarimanesh, K. Natarajan, J.O. Hahn, R. Mukkamala, PPG sensor contact pressure should Be taken into account for cuff-less blood pressure measurement, IEEE Trans. Biomed. Eng. 67 (11) (2020) 3134–3140.
[10] I. Sharifi, S. Goudarzi, M.B. Khodabakhshi, A novel dynamical approach in continuous cuffless blood pressure estimation based on ECG and PPG signals, Artif. Intell. Med. 97 (2019) 143–151.
[11] Y. Yoon, J.H. Cho, G. Yoon, Non-constrained blood pressure monitoring using ECG and PPG for personal healthcare, J. Med. Syst. 33 (4) (2009) 261–266.
[12] C.A. Haque, T.H. Kwon, K.D. Kim, Cuffless blood pressure estimation based on Monte Carlo simulation using photoplethysmography signals, Sensors 22 (3) (2022).
[13] L.D. Wang, W. Zhou, Y. Xing, X.G. Zhou, A novel neural network model for blood pressure estimation using photoplethesmography without electrocardiogram, J. Healthc. Eng. 2018 (2018) (in English).
[14] R.K. Pandey, T.Y. Lin, P.C.P. Chao, Design and implementation of a photoplethysmography acquisition system with an optimized artificial neural network for accurate blood pressure measurement, Microsyst. Technol. 27 (6) (2021) 2345–2367 (in English).
[15] G. Slapnicar, N. Mlakar, M. Lustrek, Blood pressure estimation from photoplethysmogram using a spectro-temporal deep neural network, Sensors 19 (15) (2019) (in English).
[16] D.U. Jeong, K.M. Lim, Combined deep CNN-LSTM network-based multitasking learning architecture for noninvasive continuous blood pressure estimation using difference in ECG-PPG features, Sci. Rep. 11 (1) (2021), 13539.
[17] H. Shin, S.D. Min, Feasibility study for the non-invasive blood pressure estimation based on ppg morphology: normotensive subject study, Biomed. Eng. Online 16 (1) (2017) 10.
[18] J. Martinez, K. Sel, B.J. Mortazavi, R. Jafari, Boosted-SpringDTW for comprehensive feature extraction of PPG signals, IEEE Open J Eng Med Biol 3 (2022) 78–85.
[19] S.C. Kim, S.H. Cho, Blood pressure estimation algorithm based on photoplethysmography pulse analyses, Appl Sci-Basel 10 (12) (2020) (in English).
[20] A. Hilson, "Bland-Altman plot," Radiology, vol. 231, no. 2, pp. 604; author reply 604-5, May 2004, .
[21] B.G. Francq, B. Govaerts, How to regress and predict in a Bland-Altman plot? Review and contribution based on tolerance intervals and correlated-errors-in-variables models, Stat. Med. 35 (14) (2016) 2328–2358.
[22] S.S. Mousavi, M. Firouzmand, M. Charmi, M. Hemmati, M. Moghadam, Y. Ghorbani, Blood pressure estimation from appropriate and inappropriate PPG signals using A whole-based method, Biomed. Signal Process. 47 (2019) 196–206 (in English).
[23] C.A. Haque, T.H. Kwon, K.D. Kim, Cuffless blood pressure estimation based on Monte Carlo simulation using photoplethysmography signals, Sensors 22 (3) (2022) (in English).
[24] Y. Kurylyak, F. Lamonaca, D. Grimaldi, A Neural Network-Based Method for Continuous Blood Pressure Estimation from a PPG Signal, in: 2013 Ieee International Instrumentation and Measurement Technology Conference (I2mtc), 2013, pp. 280–283 (in English)[Online]. Available: <Go to ISI>://WOS:000326900400053.
[25] X.F. Teng, Y.T. Zhang, Continuous and noninvasive estimation of arterial blood pressure using a photoplethysmographic approach, in: Proceedings of the 25th Annual International Conference of the Ieee Engineering in Medicine and Biology Society, Vols 1–4, vol. 25, 2003, pp. 3153–3156 (in English).
[26] X.M. Xing, M.S. Sun, Optical blood pressure estimation with photoplethysmography and FFT-based neural networks, Biomed. Optics Express 7 (8) (2016) 3007–3020 (in English).
[27] K.W. Chan, K. Hung, Y.T. Zhang, Noninvasive and cuffless measurements of blood pressure for telemedicine, P. Ann. Int. Ieee Embs 23 (2001) 3592–3593 (in English) [Online]. Available: <Go to ISI>://WOS:000178871900990.
[28] Y.H. Kao, P.C.P. Chao, C.L. Wey, Design and validation of a new PPG module to acquire high-quality physiological signals for high-accuracy biomedical sensing, IEEE J. Sel. Top. Quant. Electron. 25 (1) (2019) (in English).
[29] H. Shin, S.D. Min, Feasibility study for the non-invasive blood pressure estimation based on ppg morphology: normotensive subject study, Biomed. Eng. Online 16 (2017) (in English).
[30] D. Fujita, A. Suzuki, K. Ryu, PPG-based systolic blood pressure estimation method using PLS and level-crossing feature, Appl Sci-Basel 9 (2) (2019) (in English).
[31] F. Schrumpf, P. Frenzel, C. Aust, G. Osterhoff, M. Fuchs, Assessment of non-invasive blood pressure prediction from PPG and rPPG signals using deep learning, Sensors (Basel) 21 (18) (2021).
[32] M. Proenca, G. Bonnier, D. Ferrario, C. Verjus, M. Lemay, PPG-based blood pressure monitoring by pulse wave analysis: calibration parameters are stable for three months, in: Annu Int Conf IEEE Eng Med Biol Soc, vol. 2019, 2019, pp. 5560–5563.
[33] M. Weenk, S.J. Bredie, M. Koeneman, G. Hesselink, H. van Goor, T.H. van de Belt, Continuous monitoring of vital signs in the general ward using wearable devices: randomized controlled trial, J. Med. Internet Res. 22 (6) (2020) (in English).